Cancer Research

Low-Dose IFNγ Induces Tumor Cell Stemness in Tumor Microenvironment of Non–Small Cell Lung Cancer

Mengjia Song[1,2,3], Yu Ping[1,2], Kai Zhang[1,2], Li Yang[1,2], Feng Li[1,2], Chaoqi Zhang[1,2,4], Shaoyan Cheng[1,2], Dongli Yue[1,2], Nomathamsanqa Resegofetse Maimela[1,2], Jiao Qu[1,2], Shasha Liu[1,2], Ting Sun[1], Zihai Li[5], Jianchuan Xia[3], Bin Zhang[6], Liping Wang[2], and Yi Zhang[1,2]

Abstract

IFNγ is conventionally recognized as an inflammatory cytokine that plays a central role in antitumor immunity. Although it has been used clinically to treat a variety of malignancies, low levels of IFNγ in the tumor microenvironment (TME) increase the risk of tumor metastasis during immunotherapy. Accumulating evidence suggests that IFNγ can induce cancer progression, yet the mechanisms underlying the controversial role of IFNγ in tumor development remain unclear. Here, we reveal a dose-dependent effect of IFNγ in inducing tumor stemness to accelerate cancer progression in patients with a variety of cancer types. Low levels of IFNγ endowed cancer stem-like properties via the intercellular adhesion molecule-1 (ICAM1)–PI3K–Akt–Notch1 axis, whereas high levels of IFNγ activated the JAK1–STAT1–caspase pathway to induce apoptosis in non–small cell lung cancer (NSCLC). Inhibition of ICAM1 abrogated the stem-like properties of NSCLC cells induced by the low dose of IFNγ both *in vitro* and *in vivo*. This study unveils the role of low levels of IFNγ in conferring tumor stemness and elucidates the distinct signaling pathways activated by IFNγ in a dose-dependent manner, thus providing new insights into cancer treatment, particularly for patients with low expression of IFNγ in the TME.

Significance: These findings reveal the dose-dependent effect of IFNγ in inducing tumor stemness and elucidate the distinct molecular mechanisms activated by IFNγ in a dose-dependent manner.

Introduction

IFNγ is widely considered to be a crucial antitumor cytokine that is mainly produced by activated T cells, natural killer (NK), and NKT cells (1, 2). After binding to the heterodimeric IFNGR1/IFNGR2 receptor complex, IFNγ initiates the activation cascade of downstream signaling events, particularly classical JAK–STAT signaling, and the transcription of multiple IFNγ-inducible genes, both of which induce cell-cycle arrest and apoptosis in tumor cells (3). However, IFNγ signaling has paradoxically been reported to promote carcinogenesis and metastasis (4, 5) through inducing inflammatory responses (6), immunosuppression or other unknown mechanisms (7). Sustained low-level IFNγ boosted the development of several types of tumor in mouse models (8, 9). Clinically, although IFNγ has been used in many anticancer clinical trials, low-level IFNγ generated at the tumor site has been shown to increase the risk of tumor metastasis during immunotherapy (10). Unfortunately, the molecular mechanisms underlying IFNγ mediating cancer progression were not fully characterized in these previous studies. Notably, recent studies have described a close relationship between IFN γ and cancer stem cell (CSC). IFN γ are capable of inducing CSCs dormancy (11) and metastatic CSC generation (12). These studies imply that IFNγ may be involved in tumor progression through conferring tumor stemness, but the exact mechanism was not fully understood.

CSCs have been reported to play key roles in tumor initiation, metastasis, recurrence, and multidrug resistance in various cancer types (13). CSCs are a small subset of self-renewed, pluripotent, immune-privileged, high-tumorigenic, and long-living malignant cells. Persistent activation of highly conserved signaling pathways, such as the Notch, Hedgehog, and/or Wnt pathways, partially determines the stem-like properties and tumorigenicity of CSCs (14). In addition, epithelial-to-mesenchymal transition (EMT), an essential developmental process that is often activated during cancer invasion and metastasis (15), was also verified as a characteristic of CSCs. Recently, a new concept of "CSC immunology" has been established, indicating that the features of CSCs are dependent on a specialized immune-niche. Many immune factors produced in tumor niches, such as IL6, IL8, and TGFβ, endow tumor cells with stem-like properties to accelerate tumor progression (16, 17).

[1]Biotherapy Center, The First Affiliated Hospital of Zhengzhou University, Zhengzhou, China. [2]Cancer Center, The First Affiliated Hospital of Zhengzhou University, Zhengzhou, China. [3]Department of Biotherapy, Sun Yat-sen University Cancer Center, Guangzhou, China. [4]Department of Thoracic Surgery, National Cancer Center/Cancer Hospital, Chinese Academy of Medical Sciences and Peking Union Medical College, Beijing, China. [5]Department of Microbiology and Immunology, Medical University of South Carolina, Charleston, South Carolina. [6]Division of Hematology/Oncology, Department of Medicine, Robert H. Lurie Comprehensive Cancer Center, Northwestern University Feinberg School of Medicine, Chicago, Illinois.

Note: Supplementary data for this article are available at Cancer Research Online (http://cancerres.aacrjournals.org/).

M. Song and Y. Ping contributed equally to this article.

Corresponding Authors: Yi Zhang, First Affiliated Hospital of Zhengzhou University, No. 1 Jianshe Road, Zhengzhou, Henan 450052, China. Phone: 8637-1662-95320; Fax: 8637-1669-70906; E-mail: yizhang@zzu.edu.cn; and Liping Wang, wlp@zzu.edu.cn

Cancer Res 2019;79:3737–48

doi: 10.1158/0008-5472.CAN-19-0596

Intercellular adhesion molecule-1 (ICAM1), a transmembrane molecule and member of the immunoglobulin superfamily of proteins expressed by leukocytes, endothelial cells, and epithelial cells, is involved in many important processes, including leukocyte endothelial transmigration, cell signaling, cell–cell interaction, cell polarity, and tissue stability (18–21). ICAM-1 can be upregulated by lipopolysaccharide and some inflammatory cytokines, such as IFNγ and TNFα (22, 23). The protumor role of ICAM1 has been identified in various cancers (24–27), which has been recently used as a target of engineered chimeric antigen receptor T-cell therapy in advanced thyroid tumors (27) and a marker of CSCs in hepatocellular carcinoma (HCC) and esophageal squamous cell carcinoma (ESCC; refs. 24, 25). In lung cancer, ICAM1 is highly expressed in CSCs (28) and responsible for the cancer initiation and metastasis (29). These studies support a potential role of ICAM1 in modulating tumor stemness and progression.

In this study, we firstly found a dose-dependent effect of IFNγ on tumor stemness in patients with non–small cell lung cancer (NSCLC), ESCC, colorectal cancer, and HCC, indicating that low-level IFNγ in tumor microenvironment (TME) induces cancer stem properties. Then, we elucidated the molecular mechanisms underlying this effect in NSCLC cells and identified that low-level IFNγ facilitated the stem-like properties through the ICAM1–PI3K–Akt–Notch1 signaling cascade, while high-level IFNγ induced cell apoptosis through the JAK1–STAT1–caspase pathway. Moreover, the increased stem-like properties of NSCLC cells induced by low-dose IFNγ were abrogated by inhibition of ICAM1 both *in vitro* and *in vivo*. These findings identify the controversial role of IFNγ in tumor progression and clearly elucidate the distinct mechanisms underlying IFNγ influencing tumor stemness in a dose-dependent manner.

Patients and Methods

Study approval

All patients provided written informed consent. This study was conducted in accordance with the Declaration of Helsinki. Human investigations were performed after approval by the Institutional Review Board of the First Affiliated Hospital of Zhengzhou University (Approval No. 2015-LW-108; Henan Sheng, China). All animal procedures were carried out according to the Guide for the Care and Use of Laboratory Animals and were approved by the Institutional Animal Care and Use committee of the First Affiliated Hospital of Zhengzhou University (Approval No. 00015613; Henan Sheng, China).

Patients and tumor samples

For IHC and immunofluorescence (IF) staining, a total of 86 NSCLC tissues were collected from the First Affiliated Hospital of Zhengzhou University from 2012 to 2014. All patients received four cycles of cisplatin-based chemotherapy after surgery without receiving any therapeutic intervention before surgery. For flow cytometry, 35 pairs of NSCLC tissues and their adjacent normal tissues were freshly obtained from the First Affiliated Hospital of Zhengzhou University from January to May 2017. For isolation of interstitial fluid, 9 fresh NSCLC tissues, 9 fresh ESCC tissues, 11 fresh colorectal cancer tissues, and 13 fresh HCC tissues were collected from the First Affiliated Hospital of Zhengzhou University. All samples in the study were confirmed by pathologic analysis.

NSCLC cell lines and cell culture

The NSCLC cell lines, A549 and H460, were purchased from the Chinese Academy of Sciences Cell Repertoire in Shanghai, China in 2017 and maintained in RPMI1640 (HyClone) supplemented with 10% FBS (HyClone), 100 U/mL of penicillin, and 100 μg/mL of streptomycin. A549 and H460 were used within 15 passages. Short tandem repeat Multi-Amplification Kit (Microreader21 ID System) was used for PCR amplification and PCR products were detected by ABI 3130xl DNA Analyzer (Applied Biosystems). *Mycoplasma* Stain Assay Kit (Beyotime Institute of Biotechnology, Beijing, China) was used for *Mycoplasma* detection. The methods of low- or high-dose IFNγ treatment for 6 days in A549 and H460 cells were as follows: recombinant human IFNγ (PeproTech) was added and cultured for 2 days, and restimulated at days 3 and 5, for a total of 6 days of treatment. Inhibition and blockade treatment were as follows: anti-IFNγ antibody (R&D Systems lnc.), inhibitors, including silibinin (Sigma), PF04691502, AZD5363, LY3039478, ruxolitinib, fludarabine, and Z-VAD-FMK (Selleck Chemicals) were pretreated for 1 hour following IFNγ treatment, which were replicated at days 3 and 5, for a total of 6 days of treatment.

Isolation of interstitial fluid from fresh tumor tissues

Fresh tissues were placed on triple-layered 10-μm nylon mesh and spun at $<50 \times g$ for 5 minutes to remove surface liquid. Next, samples were centrifuged at $400 \times g$ for 10 minutes to isolate the tumor interstitial fluid (TIF; ref. 30).

In vivo metastatic growth model

Twenty-four 5-week-old female NOD-SCID mice were randomly divided into six groups ($n = 5$ each). Luciferase-shScramble–infected, luciferase-shICAM1#1–infected, and luciferase-shICAM1#3–infected cells were pretreated with PBS or low-dose IFNγ (0.1 ng/mL) *in vitro* for 6 days and then intravenously injected into the lateral tail vein of mice (5×10^6 cells in 100-μL PBS). Metastasis was evaluated using an *in vivo* imaging system at day 0, 6, 12, and 18 after injection. The lungs of the mice in each group were harvested to analyze the frequency of GFP^+ NSCLC cells by flow cytometry and the metastatic nodules by hematoxylin–eosin staining.

Chromatin immunoprecipitation assay

The chromatin immunoprecipitation (ChIP) assay was performed according to the manufacturer's instructions (Cell Signaling Technology). Anti-N1ICD (Cell Signaling Technology 1:200) or anti-RBP-Jκ (Cell Signaling Technology, 1:50) antibody was used to immunoprecipitate the chromatin in A549 and H460 cells transfected with shScramble or with shScramble, shICAM1#1, or shICAM1#3 following low-dose IFN γ treatment. RT-PCR was performed using primers identified for the RBP-Jκ-binding site in the *CD133* promoter region as follows: 5′- AGAGACTTCG-GACTCGCTCT -3′, 5′- CACAGTGTTGGCCCATTTCC -3′.

Statistical analysis

Data are shown as the mean ± SD and analyzed using Student *t* test or χ^2 test. A paired *t* test was used for paired samples. Survival curves were plotted using the Kaplan–Meier method. Differences in survival times among the patient subgroups were analyzed by the log-rank test. Cox proportional hazard regression model was used to evaluate the prognostic value of the risk factors. Statistical analyses were performed using GraphPad Prism 7 and SPSS

software (GraphPad software). A value of $P < 0.05$ was considered statistically significant.

Results

Low-level IFNγ expression is closely associated with poor prognosis and increased expression of CSC markers in patients with NSCLC

IFNγ is known as a representative antitumor cytokine in the TME (1). We firstly detected the source of IFNγ in 5 fresh tumor tissues from patients with NSCLC by flow cytometry. $CD3^+CD8^+$ T cells, $CD3^+CD4^+$ T cells, NK cells, and NKT cells showed high production of IFNγ, while $CD3^+CD4^+Foxp^+$ Treg cells showed low production (Supplementary Fig. S1A and S1B). Importantly, $CD3^+CD8^+$T cells were identified as the main source of IFNγ with an average of 83.82% in IFNγ-positive subset (Supplementary Fig. S1C). IHC staining analysis showed a significantly positive correlation between IFNγ and CD8 expression in 35 patients with NSCLC, indicating IFNγ level was strongly associated with $CD8^+$ tumor-infiltrating lymphocytes (TIL; Supplementary Fig. S1D and S1E). Next, the actual distribution pattern of IFNγ in 86 NSCLC tissues was also investigated by IHC staining (Fig. 1A). Interestingly, we found that low-level IFNγ expression accounted for the majority in NSCLC tissues (Fig. 1B). Moreover, low-level IFNγ expression was strongly correlated with the TNM stage, brain metastasis, and chemoresistance (Supplementary Table S1). Shorter overall survival (OS) and progression-free survival (PFS) time were also observed in low-level IFNγ group than both negative and high-level IFNγ group (Fig. 1C and D). In addition, the univariate and multivariate Cox regression analyses indicated IFNγ expression level was an independent prognostic factor for the OS of patients with NSCLC (Table 1; Supplementary Table S2). Taken together, these results suggest that low-level IFNγ in the TME may play a role in NSCLC progression.

CSCs have been reported to participate in tumor initiation, metastasis, recurrence, and multidrug resistance (13), serving as a key mechanism of tumor progression. CD133 has been identified as a marker of CSCs in NSCLC (31, 32). As CSCs are also characterized by enhanced EMT (15), vimentin, an EMT marker, was used as another CSC marker in our study. By IF staining, we intriguingly found much higher expression of CD133 and vimentin on tumor cells in IFNγ-low TME than that in IFNγ-high TME in NSCLC tissues (Fig. 1E and F). A significantly negative correlation between IFNγ and CD133 or vimentin was observed by IHC staining analysis in 86 NSCLC tissues (Fig. 1G and H). In addition, a negative correlation between IFNG and PROM1 was also observed in lung adenocarcinoma collected from The Cancer Genome Atlas (TCGA; Supplementary Fig. S2A). To further accurately quantify the level of IFNγ promoting tumor stemness, we performed ELISA to detect the concentration of IFNγ in TIF isolated from fresh 9 NSCLC tissues. Accordingly, cancer stem properties were evaluated by the percentage of $CD133^+$ stem cells in $CD326^+$ tumor cells and the expression of stemness-related genes. Intriguingly, we found patients with relative low-level (around 0.137 ng/mL) IFNγ in TIF showed increased cancer stem properties, and patient #4 with 0.110 ng/mL IFNγ showed the highest percentage $CD133^+$ stem cells and highest expression of most stemness-related genes. However, patients with high-level IFNγ in TIF showed decreased stem-like properties (Fig. 1I). We also found similar results in tumor tissues from patients with ESCC, colorectal cancer, and HCC, whose low-level border of IFNγ correlated with highest stem-like properties was 0.072, 0.152, and 0.118 ng/mL, respectively (Supplementary Fig. S2B–S2D). Therefore, we preliminarily surmise that the low-level IFNγ may serve as a key determinant inducing tumor stemness.

Low-dose IFNγ augments the stem-like properties of NSCLC cells

To clarify the role of low-level IFNγ in inducing tumor stemness, NSCLC cell lines, A549 and H460 cells, were treated with different doses of recombinant human IFNγ for 1–6 day(s). As expected, progressively increasing apoptosis and decreasing proliferation were observed with the increase of IFNγ dose and treatment time (Fig. 2A; Supplementary Fig. S3A and S3B). Strikingly, we found that the frequency of Annexin V^-CD133^+ cells was significantly increased over time after treated with a relatively low-dose IFNγ ($\leq$0.2 ng/mL; Fig. 2B; Supplementary Fig. S3C). Almost consistent with the concentration of IFNγ (0.110 ng/mL) corresponding to the highest cancer stem properties in the TIF of patients with NSCLC (Fig. 1I), the *in vitro* optimal concentration of IFNγ inducing Annexin V^-CD133^+ cells was 0.1 ng/mL (Fig. 2B; Supplementary Fig. S3C). However, after treating with a relatively high dose of IFNγ ($\geq$100 ng/mL), the percentage of Annexin V^-CD133^+ cells turned to decrease over time (Fig. 2B). On the basis of the clinical and *in vitro* results, we preliminarily speculated that low-dose and long-term IFNγ stimulation might enhance the stem-like properties of NSCLC cells. To validate this conception, we next sorted the Annexin V^- NSCLC cells treated with either low-dose (0.1 ng/mL) or high-dose (100 ng/mL) IFNγ to examine their sphere-forming ability. Significantly increased sphere number was observed in the low-dose IFNγ treatment group compared with the control and the high-dose IFNγ treatment groups (Fig. 2C). Similar results were also found in the expression of CSC markers (Fig. 2D) and CSC signature genes (Fig. 2E). Because high tumorigenicity is a key characteristic of CSCs, we additionally explored the effect of low dose of IFNγ on tumor growth in NSCLC xenograft models. A549 cells stably expressing luciferase were injected subcutaneously into BABL/c nude mice and then intratumorally treated with PBS or different doses of IFNγ. Interestingly, we found that both tumor volumes (Fig. 2F and G) and the frequency of $CD133^+$ tumor cells in xenografts (Fig. 2H) were dramatically increased following low-dose (0.1 μg/day), but decreased following high-dose (10 μg/day) IFNγ administration. Taken together, these results suggest that low dose of IFNγ facilitates the stem-like properties of NSCLC cells both *in vitro* and *in vivo*.

ICAM1 is crucial for the increased stem-like properties of NSCLC cells induced by low-dose IFNγ

To understand the molecular mechanism underlying low dose of IFNγ inducing the stem-like properties in NSCLC cells, we searched the IFNγ signaling downstream genes using the GCBI website (https://www.gcbi.com.cn/) and evaluated the different expression levels of these genes by RT-PCR in A549 and H460 cells treated with or without low dose of IFNγ. Most of these genes, including IFNGR1 and IFNGR2, were significantly upregulated (Fig. 3A). Among them, ICAM1 showed the most obvious gene upregulation in response to low dose of IFNγ (Fig. 3A), which was further confirmed by flow cytometry (Fig. 3B). After neutralization with anti-IFNγ antibody, ICAM1 (Supplementary Fig. S4A) expression was efficiently blocked, as well as IFNGR1 and IFNGR2 (Supplementary Fig. S4B and S4C). ICAM1 is a transmembrane

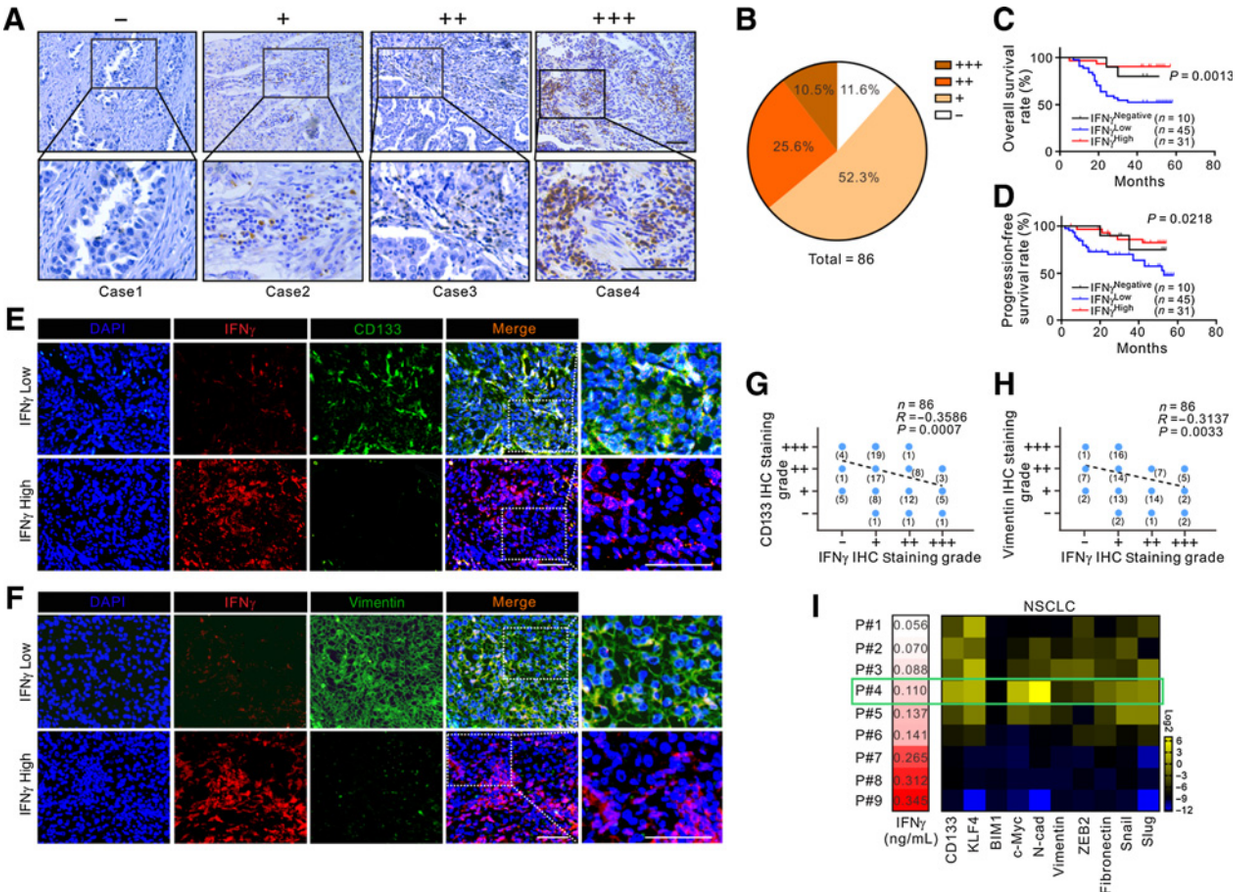

Figure 1.

Low-level IFNγ expression is correlated with tumor stemness in patients with NSCLC. **A,** Representative photomicrographs of IHC staining for IFNγ in NSCLC tissues. Scale bars, 100 μm. **B,** Real distribution of IHC results of IFNγ in 86 NSCLC tissues. **C** and **D,** Kaplan–Meier analysis of OS and PFS in 86 patients with NSCLC according to different IFNγ levels in NSCLC tissues by IHC staining. **E** and **F,** IF staining of the colocalization of IFNγ (red) with CD133 (green) or vimentin (green) in NSCLC tissues. Colocalization, yellow. DAPI, blue. Figure panel pairs represent images taken with different zooming options; scale bars, 100 μm. **G** and **H,** Spearman correlation analysis was performed to analyze the correlation between IFNγ and CD133 and vimentin according to the IHC staining results. **I,** Heatmap showed the expression of IFNγ and stemness-related genes. Left, the concentration of IFNγ in TIF was detected by ELISA. Right, the percentage of CD133-positive cells in tumor cells, which was labeled by CD326 positive, was detected by flow cytometry and the expression of other stemness-related genes was tested by RT-PCR in NSCLC. Patient #4 labeled by green frame showed the highest expression of stemness-related genes. Log-rank tests were used in **C** and **D**. The results are representative of three independent experiments.

molecule that stabilizes cell–cell interactions and enhances transendothelial transmigration (20, 21). In NSCLC cells, we observed an obvious upregulation of ICAM1 in CSCs generated by nonadhesive culture system (Supplementary Fig. S5), suggesting a potential role of ICAM1 in mediating NSCLC stemness and metastasis. Moreover, IF colocalization analysis demonstrated that ICAM1 was coexpressed with CD133 and vimentin in A549 cells, which was dramatically increased by low-dose IFNγ (Fig. 3C). On the basis of these results, we hypothesized that ICAM1 might be essential for low-dose IFNγ inducing the stem-like properties in NSCLC cells.

To test this hypothesis, silibinin, a pharmacologic inhibitor of ICAM1, was added to A549 and H460 cells following treatment with low dose of IFN γ. Interestingly, we found silibinin partially abrogated the sphere-forming ability (Fig. 3D) and the expression of CSC markers (Fig. 3E) and CSC signature genes (Fig. 3F) in NSCLC cells treated with low dose of IFNγ. Next, we stably knocked down ICAM1 expression in A549 and H460 cells with shICAM1s viruses (Fig. 3G). As expected, ICAM1 knockdown remarkably reduced the stem-like properties induced by low-dose IFNγ (Fig. 3G–I). Taken together, these results indicate that low dose of IFNγ drives ICAM1 expression to mediate the stem-like properties of NSCLC cells.

Activation of the PI3K–Akt–Notch1 pathway by ICAM1 in NSCLC cells is required for low-dose IFNγ-induced stem-like properties

Next, we explored the signaling pathways involved in the stem-like properties driven by low dose of IFNγ. We chose several CSC-relevant signaling activation inhibitors, including PI3K, Akt, Notch1, STAT3, p38, and ERK1/2 inhibitors, to pretreat A549 and H460 cells following low-dose IFNγ treatment. Intriguingly, the RT-PCR results showed that none of the inhibitors had an obvious effect on ICAM1 expression compared with DMSO, but

Table 1. Multivariate Cox regression analysis of clinicopathologic factors for OS in patients with NSCLC

	OS			
	Univariate Cox		Multivariate Cox	
Variable	*P*	HR	*P*	HR
Age				
≥55 or <55	0.6863	1.1941	0.8767	0.9249
Gender				
Male or female	0.9685	0.9835	0.7441	0.8296
Smoking history				
Yes or no	0.1473	0.5668	0.506	1.4857
Grade				
Low, medium, or high	0.9619	1.0166	0.7709	1.1175
Histology				
Adenocarcinoma or squamous cell carcinoma	0.5867	0.8082	0.1138	0.406
TNM stage				
I/II or III/IV	0.8337	1.0926	0.678	0.7535
Lymph node metastasis				
Yes or no	0.2408	1.5759	0.1748	2.113
Bone metastasis				
Yes or no	0.9406	0.9605	0.8856	0.8884
Brain metastasis				
Yes or no	0.0001	6.1131	0.0614	6.4732
EGFR mutation				
Yes or no	0.0108	2.716	0.0725	2.1572
Chemoresistance				
Yes or no	0.0221	2.4962	0.9522	0.9506
IFNγ expression				
Negative/low or high	0.0054	0.1815	0.0219	0.1985

NOTE: $P < 0.05$, significant.

PF04691502, AZD5363, and LY3039478 partially reversed the elevated stem-like properties of A549 and H460 cells (Fig. 4A and B). Similar results were also observed in the flow cytometry and Western blot analyses, which demonstrated that PF04691502, AZD5363, and LY3039478 did not affect ICAM1 expression but dramatically blocked the increased expression of CSC markers compared with DMSO in A549 and H460 cells treated with low-dose IFNγ (Fig. 4C and D). Therefore, we hypothesized that the PI3K–Akt and Notch1 pathways might act as the downstream signaling pathways of ICAM1 to participate in low dose of IFNγ inducing the stem-like properties in NSCLC cells. The next Western blot analysis demonstrated a significantly upregulated activation of Akt and Notch1 after low-dose IFNγ treatment in contrast to the control, whereas inhibition of ICAM1 by silibinin or ICAM1 shRNAs could efficiently impair their activation (Fig. 4E and F), indicating that ICAM1 activates the PI3K–Akt and Notch1 pathways to mediate the stem-like properties of NSCLC cells treated with low-dose IFNγ.

Then, we assessed the activation of the PI3K–Akt and Notch1 pathways in NSCLC cells pretreated with DMSO, PI3K, Akt, and Notch1 signaling activation inhibitors following low-dose IFNγ stimulation. As shown in Fig. 4D, compared with DMSO, PF04691502 and AZD5363 pretreatment reduced the activation of both Akt and Notch1, while LY3039478 pretreatment only attenuated Notch1 activation but did not affect Akt activation. These results suggest that Notch1 is the downstream pathway of the PI3K–Akt pathway in NSCLC cells treated with low-dose IFNγ.

Upon activation, the Notch1 receptor is cleaved and subsequently releases the Notch1 intracellular domain (N1ICD), which migrates into the nucleus and forms a complex with the nuclear proteins of the RBP-Jκ family. RBP-Jκ acts as a transcriptional activator to activate the expression of target genes after forming a complex with N1ICD (33). We next used the PROMO website to predicate putative RBP-Jκ–binding sites in the *CD133* promoter region and identified an RBP-Jκ–binding site in the −156 to −145 region (Fig. 4G). ChIP assays were performed to validate whether the RBP–Jκ–NICD complex bound to the putative site. As shown in Fig. 4H and I, RBP-Jκ and NICD bound directly to the putative RBP-Jκ–binding site in the *CD133* promoter region in A549 and H460 cells, which showed an increase in shScramble cells treated with low-dose IFNγ but a decrease in shICAM#1 and shICAM1#3 cells treated with low-dose IFNγ compared with shScramble cells. These data suggest that Notch1 directly regulates *CD133* transcription in NSCLC cells.

High-dose IFNγ contributes to apoptosis through activation of the JAK1–STAT1–caspase signaling pathway in NSCLC cells

Above data revealed that low dose of IFNγ promoted the stem-like properties of NSCLC cells through activation of the ICAM1–PI3K–Akt–Notch1 axis. However, high dose of IFNγ was found to induce apoptosis and decrease the stem-like properties of NSCLC cells, as shown in Fig. 2, which prompted our interest in the signaling pathways involved in the high-dose IFNγ treatment system. The JAK1–STAT1–caspase pathway has been previously described as the key downstream pathway of IFNγ-mediated apoptosis (3), and our results indicated that the ICAM1–PI3K–Akt–Notch1 axis was the key signaling cascade in IFNγ-mediated stem-like properties. Therefore, we next examined the activation of the JAK1–STAT1–caspase pathway and ICAM1–PI3K–Akt–Notch1 axis in NSCLC cells treated with either low-dose or high-dose IFNγ, respectively. The results showed that cells treated with high-dose IFNγ exhibited much higher activation of JAK1, STAT1, caspase 3, and caspase 7 than those treated with low-dose IFNγ (Fig. 4J). Surprisingly, we further observed a significant decrease in the activation of Akt and Notch1 in cells treated with high-dose IFNγ compared with those treated with low-dose of IFNγ, although both high-dose and low-dose IFNγ were able to induce high levels of ICAM1 expression (Fig. 4J). Thus, high-dose IFNγ promoted apoptosis of NSCLC cells through the JAK1–STAT1–caspase pathway, whereas high-dose IFNγ-induced ICAM1 was insufficient to endow the stem-like properties of NSCLC cells through the PI3K–Akt–Notch1 signaling pathway.

Next, we wondered whether ICAM1 played a role in high-dose IFNγ-mediated apoptosis. After treatment with different doses of IFNγ, we found that ICAM1 knockdown had no influence on apoptosis in A549 and H460 cells (Fig. 4K), while activation of JAK1, STAT1, caspase 3, and caspase 7 was increased with the increase of IFNγ dose (Fig. 4L). Moreover, inhibition of JAK1 (ruxolitinib), STAT1 (fludarabine), and caspase (Z-VAD-FMK) significantly attenuated high-dose IFNγ-mediated apoptosis (Fig. 4M). Western blot analysis showed that phospho-JAK1 expression was only inhibited by ruxolitinib and phosoho-STAT1 expression was inhibited by both ruxolitinib and fludarabine, while caspases 3 and 7 were inhibited by ruxolitinib, fludarabine, and Z-VAD-FMK (Fig. 4N). These data indicate that high-dose IFNγ promotes apoptosis of NSCLC cells by activating the JAK1–STAT1–caspase signaling pathway in an ICAM1-independent manner.

ICAM1 knockdown reverses tumor growth induced by low-dose IFNγ in xenograft model of NSCLC

To identify whether ICAM1 played a role in low-dose IFNγ-induced tumor growth, A549 cells stably expressing luciferase

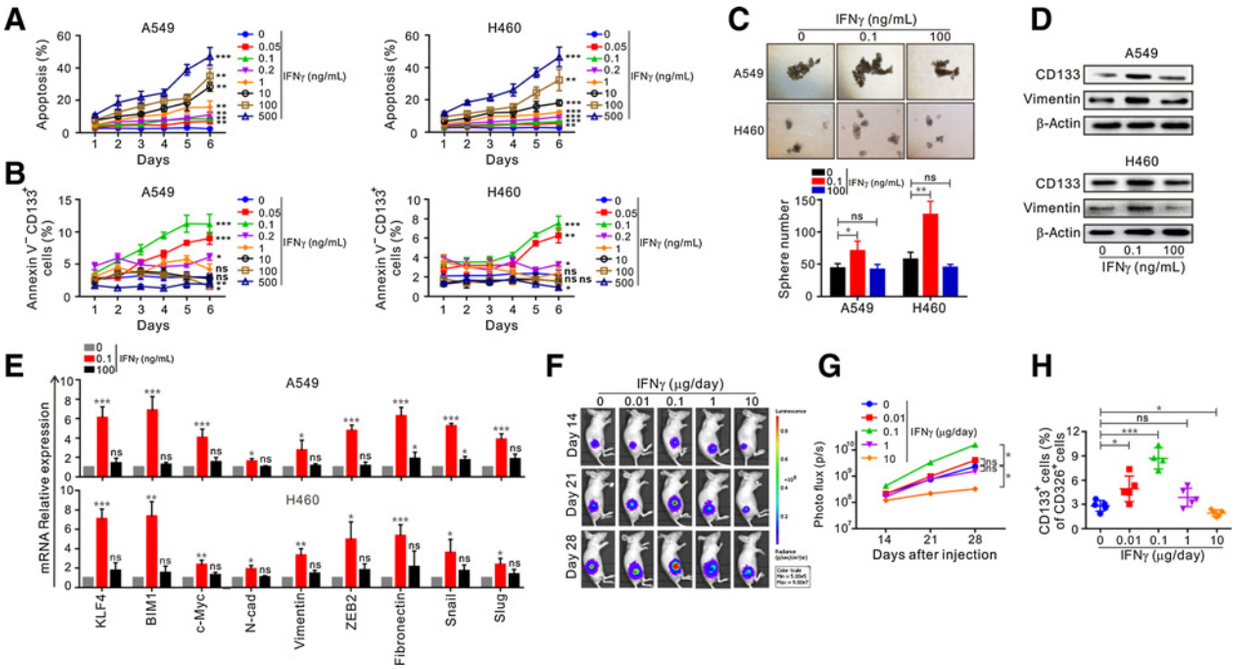

Figure 2.

Low-dose IFNγ augments the stem-like properties of NSCLC cells. A549 and H460 cells were treated with different doses of recombinant human IFNγ for 1–6 days. **A,** The frequency of apoptotic A549 (left) and H460 (right) cells labeled with Annexin V^+PI^- or Annexin V^+PI^+ was examined by flow cytometry. **B,** The frequency of Annexin V^-CD133^+ A549 (left) and H460 (right) cells was examined by flow cytometry. **C–E,** Annexin V^- A549 and H460 cells treated with either low (0.1 ng/mL) or high (100 ng/mL) dose of IFNγ for 6 days were then sorted using flow cytometry. **C,** The sphere-forming assay. **D,** Expression of CD133 and vimentin in A549 (top) and H460 (bottom) cells was detected by Western blotting. **E,** The expression of CSC signature genes in A549 (left) and H460 (right) cells was detected by RT-PCR. **F–H,** A549 cells stably expressing luciferase were injected subcutaneously into nude mice. PBS or different doses of IFNγ were intratumorally injected from day 14 to 28. **F** and **G,** Tumor volumes were measured at day 14, 21, and 28 by *in vivo* imaging system. **H,** The frequency of $ICAM1^+CD133^+$ tumor cells in mouse-bearing xenografts was detected by flow cytometry. The results are representative of three independent experiments. *, $P < 0.05$; **, $P < 0.01$; ***P, < 0.001; ns, nonsignificant.

were injected subcutaneously into BALB/c nude mice. The mice were treated intratumorally with PBS or low-dose IFNγ, and silibinin was orally administered. We found that the enhanced tumor growth induced by low-dose IFNγ was efficiently blocked by silibinin (Supplementary Fig. S6A and S6B). Silibinin also dramatically reduced the high frequency of $ICAM1^+CD133^+$ tumor cells in xenografts treated with low-dose IFNγ (Supplementary Fig. S6C).

In Fig. 3F and G, we had confirmed that low dose of IFNγ promoted NSCLC growth via ICAM1 in BABL/c nude mice. Next, NOD-SCID mice were used as another model to evaluate the protumor effect of low-dose IFNγ and the role of ICAM1 during this process. Luciferase-shScramble–infected, luciferase-shICAM1#1–infected, and luciferase-shICAM1#3–infected cell lines were stably established and injected subcutaneously into NOD-SCID mice. The mice in each group were further intratumorally treated with PBS or low-dose IFNγ. We found tumor growth of shICAM1#1 cell–derived and shICAM1#3 cell–derived xenografts was significantly reduced compared with shScramble cell–derived ones (Fig. 5A and B). Moreover, a remarkable increase of tumor growth was detected in shScramble cell–derived xenografts after treatment with low-dose IFNγ, while shICAM1#1 and shICAM1#3 cell–derived xenografts did not exhibit obvious differences after low-dose IFNγ treatment (Fig. 5A and B). Besides, low-dose IFNγ treatment greatly enhanced the frequency of $ICAM1^+CD133^+$ tumor cells in shScramble cell–derived xenografts, but had no significant effect on those in shICAM1#1 and shICAM1#3 cell–derived xenografts (Fig. 5C). Similar results were obtained for the expression of ICAM1, CD133, and vimentin by IHC staining (Fig. 5D-G). Taken together, these data indicate that ICAM1 is essential for low-dose IFNγ-mediated tumor growth in immunodeficient mice.

Low-dose IFNγ facilitates NSCLC cell metastatic growth in murine lungs via ICAM1

Apart from the high sphere-forming ability and high tumorigenicity, CSCs can also form a hierarchy of stem-like and differentiated tumor cells to initiate metastatic growth (16). Therefore, we investigated the effect of low-dose IFNγ on the metastatic growth of NSCLC cells and the role of ICAM1 in this process. Before intravenous injection into the lateral tail vein of NOD-SCID mice, luciferase-shScramble–infected, luciferase-shICAM1#1–infected, and luciferase-shICAM1#3–infected cells were pretreated with PBS or low-dose IFNγ for 6 days *in vitro*, and the percentage of $CD133^+$ cells was shown in Supplementary Fig. S7. After intravenous injection, we observed that luciferase-shScramble–infected cells pretreated with low-dose IFNγ generated larger lung metastatic nodules than luciferase-shScramble–infected cells pretreated with PBS, whereas luciferase-shICAM1#1- and shICAM1#3–infected cells pretreated with low-dose IFNγ did not show significant difference compared with those pretreated

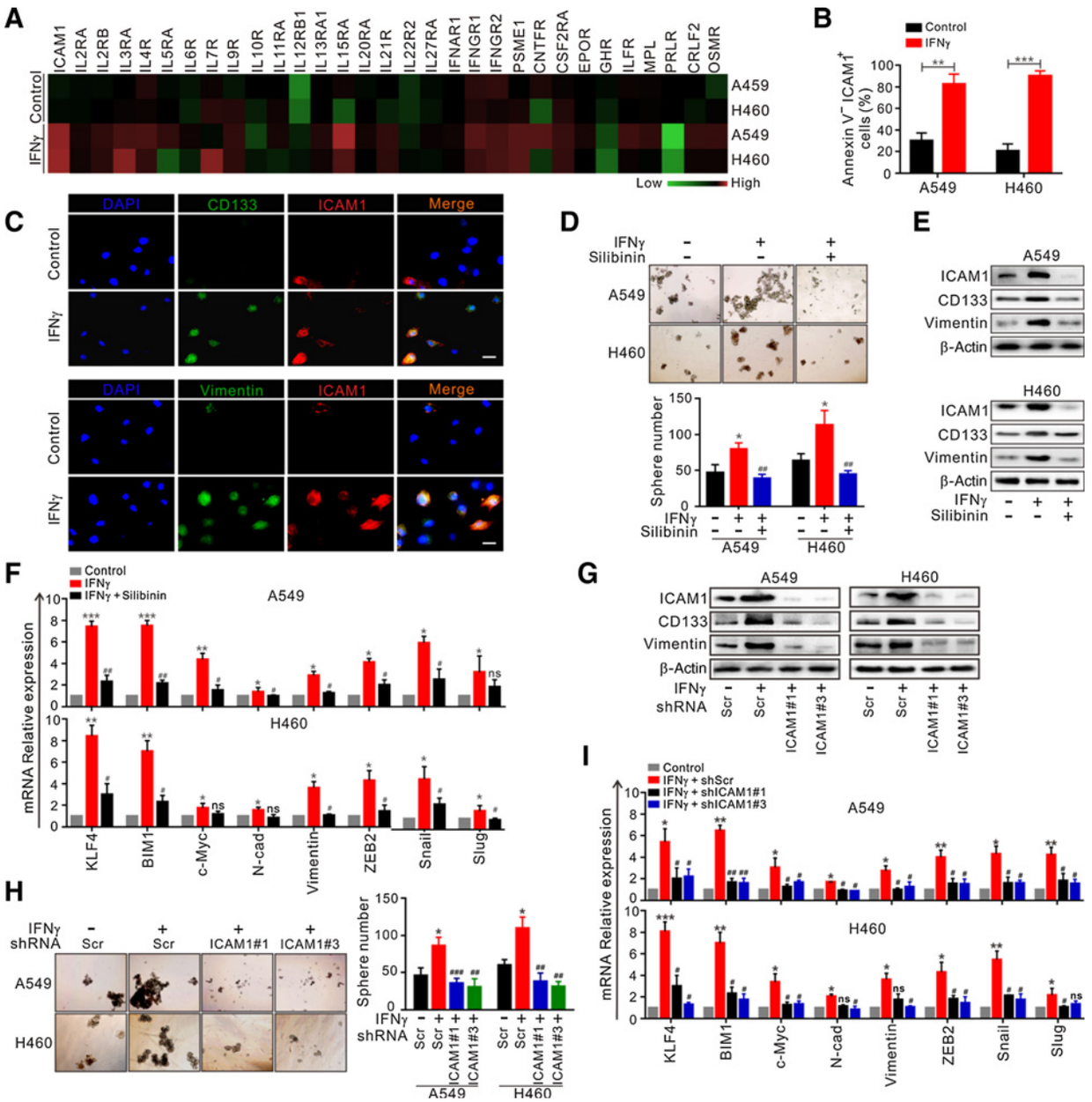

Figure 3.

ICAM1 mediates low-dose IFNγ-induced stem-like properties of NSCLC cells. **A,** The expression of IFNγ signaling downstream genes in A549 and H460 cells treated with or without low-dose IFNγ (0.1 ng/mL) for 6 days was detected by RT-PCR. **B,** The frequency of Annexin V$^-$ICAM1$^+$ cells was detected by flow cytometry. **C,** IF staining for the colocalization of ICAM1 (red) with CD133 (green, top) or vimentin (green, bottom) in A549 cells treated with or without low-dose IFNγ (0.1 ng/mL) for 6 days was performed, and the colocalization is indicated in yellow. DAPI, blue. Scale bars, 20 μm. **D–F,** A549 and H460 cells were treated with or without silibinin (100 μmol/L) following low-dose IFNγ (0.1 ng/mL) treatment. Sillibnin and IFNγ treatment was replicated at day 3 and 5, for a total of 6 days of treatment. **D,** The sphere formation assay in A549 (top) and H460 (bottom) cells. **E,** The expression of CD133 and vimentin in A549 (top) and H460 (bottom) cells was detected by Western blotting. **F,** The expression of CSC signature genes in A549 (top) and H460 (bottom) cells was detected by RT-PCR. **G–I,** A549 and H460 cells were transfected with shScramble, shICAM1#1, or shICAM1#3 following low-dose IFNγ (0.1 ng/mL) treatment for 6 days. **G,** The expression of CD133 and vimentin in A549 (left) and H460 (right) cells was examined by Western blotting. **H,** The sphere-forming assay. **I,** RT-PCR was used to detect the mRNA expression of CSC signature genes in A549 (top) and H460 (bottom) cells. The results are representative of three independent experiments. *, $P < 0.05$; **, $P < 0.01$; ***, $P < 0.001$; $^{\#}$, $P < 0.05$; $^{\#\#}$, $P < 0.01$; $^{\#\#\#}$, $P < 0.001$; ns, nonsignificant. Scr, Scramble.

with PBS (Fig. 5H and I). In the PBS-pretreated groups, mice injected with luciferase-shICAM1#1- and shICAM1#3–infected cells had smaller lung metastatic nodules than those injected with luciferase-shScramble–infected cells (Fig. 5H and I). Consistently, similar results were also obtained in the frequency of GFP$^+$ NSCLC cells (Fig. 5J) and the percentage of metastatic cancerous

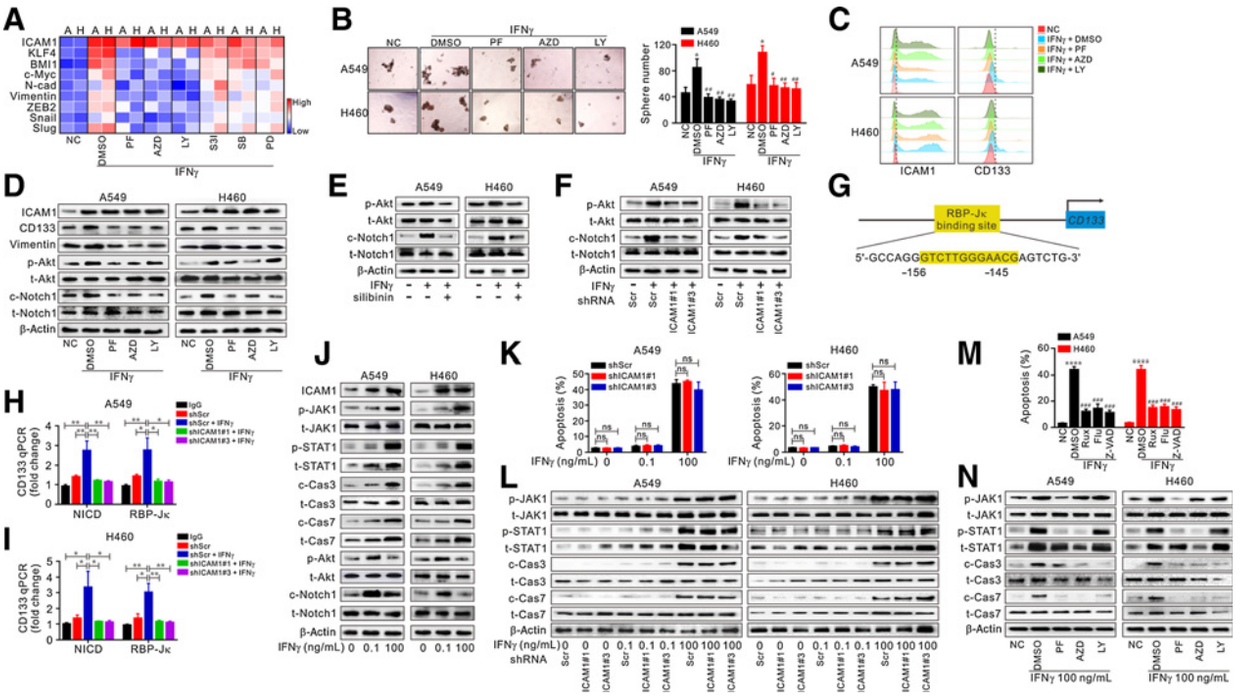

Figure 4.

Activation of the ICAM1–PI3K–Akt–Notch1 axis and JAK1—STAT1–caspase pathway is responsible for low-dose IFNγ–induced stemness and high-dose-IFNγ–mediated apoptosis in NSCLC cells, respectively. **A–D**, **M**, and **N,** A549 and H460 cells were pretreated with DMSO, PF04691502 (1 μmol/L), AZD5363 (10 μmol/L), LY3039478 (50 μmol/L), S3I-201 (20 μmol/L), SB203580 (10 μmol/L), PD98059 (20 μmol/L), ruxolitinib (1 μmol/L), fludarabine (1 μmol/L), or Z-VAD-FMK (40 μmol/L) following low (0.1 ng/mL) or high (100 ng/mL) dose IFNγ treatment. Inhibition treatment and IFNγ treatment were replicated at days 3 and 5, for a total of 6 days of treatment. **A,** The mRNA expression of ICAM1 and CSC signature genes was tested by RT-PCR. **B,** The sphere-forming assay. **C,** Flow cytometry was used to test the expression of ICAM1 (left) and CD133 (right). **D,** Western blot analysis was used to assess the expression of ICAM1, CD133, vimentin, phospho-Akt, total-Akt, cleaved-Notch1, and total-Notch1. **E** and **F,** The expression of phospho-Akt, cleaved-Notch1, and their total proteins was tested by Western blotting. **G,** Analysis of the *CD133* promoter identified an RBP-Jκ–binding site. **H** and **I,** ChIP was performed using IgG, anti-NICD, or anti-RBP-Jκ antibody, followed by quantitative RT-PCR. **J,** The expression of ICAM1, phospho-JAK1, phospho-STAT1, cleaved caspase-3, cleaved caspase-7, phospho-Akt, cleaved Notch1, and their total proteins was tested by Western blotting. **K** and **L,** Cells were treated with 0, 0.1 and 100 ng/mL IFNγ for 6 days. **K** and **M,** Flow cytometry was used to test apoptosis. **I** and **N,** Western blot analysis was performed to examine the expression of phospho-JAK1, phospho-STAT1, cleaved caspase-3, cleaved caspase-7, and their total proteins. The results are representative of three independent experiments. In **B** and **M**, *, $P < 0.05$; ****, $P < 0.0001$ versus negative control group; $^{\#}$, $P < 0.05$; $^{\#\#}$, $P < 0.01$; $^{\#\#\#}$, $P < 0.001$ versus IFNγ or IFNγ plus DMSO group. In **H** and **I**, *, $P < 0.05$; **, $P < 0.01$. A, A549; H, H460; NC, negative control; ns, not significant; Scr, Scramble.

areas in the lungs of mice (Fig. 5K). Together, these results suggest that low-dose IFNγ greatly enhances lung metastasis of NSCLC cell *in vivo*, which is mediated by ICAM1.

The expression level of ICAM1 is significantly upregulated by CD133^{+} tumor cells and positively correlated with a poor prognosis in patients with NSCLC

Subsequently, we detected the expression level of ICAM1 in clinical samples. Flow cytometry analysis demonstrated higher ICAM1 expression by tumor cells from tumor tissues than epithelial cells from adjacent normal tissues in patients with NSCLC (Fig. 6A). A dramatically elevated frequency of ICAM1^{+} cells in CD133^{+} tumor cells was also observed compared with CD133^{-} tumor cells (Fig. 6B). Data from the TCGA database revealed a close association of ICAM1 with CSC-related genes at the mRNA level in 1,016 NSCLC tissues (Supplementary Fig. S8A–S8G). Consistently, the IHC staining results demonstrated strongly positive correlation of ICAM1 with CD133 (Fig. 6E) and vimentin (Fig. 6F) in 86 NSCLC tissues. Moreover, coexpression of ICAM1 with CD133 and vimentin was found in NSCLC tissues, and the coexpression levels in chemoresistant patients were significantly higher than those in chemosensitive patients (Supplementary Fig. S8H). These data suggest that ICAM1 may be a malignant signature of NSCLC cells.

On the basis of the IHC staining of ICAM1, a significant correlation was found between ICAM1 expression and TNM stage, bone metastasis, EGFR mutation, and chemoresistance (Supplementary Table S3). Patients with high-level ICAM1 had a worse OS (Fig. 6G) and PFS (Fig. 6H). Data from TCGA also showed that high-level ICAM1 was strongly associated with a poor PFS in patients with NSCLC (Supplementary Fig. S8I). These data suggest that ICAM1 is strongly associated with prognosis in patients with NSCLC. In addition, we further stratified the 86 NSCLC tissues into four groups according to the expression levels of IFNγ and ICAM1 analyzed by IHC staining: IFNγ^{low}ICAM1^{low}, IFNγ^{low}ICAM1^{high}, IFNγ^{high}ICAM1^{low}, and IFNγ^{high}ICAM1^{high}. Surprisingly, we found that patients with IFNγ^{high}ICAM1^{high} expression showed a better OS (Fig. 6I) and PFS (Fig. 6J) than those with IFNγ^{low}ICAM1^{high} expression, which supported the view that ICAM1 might mediate tumor progression or even

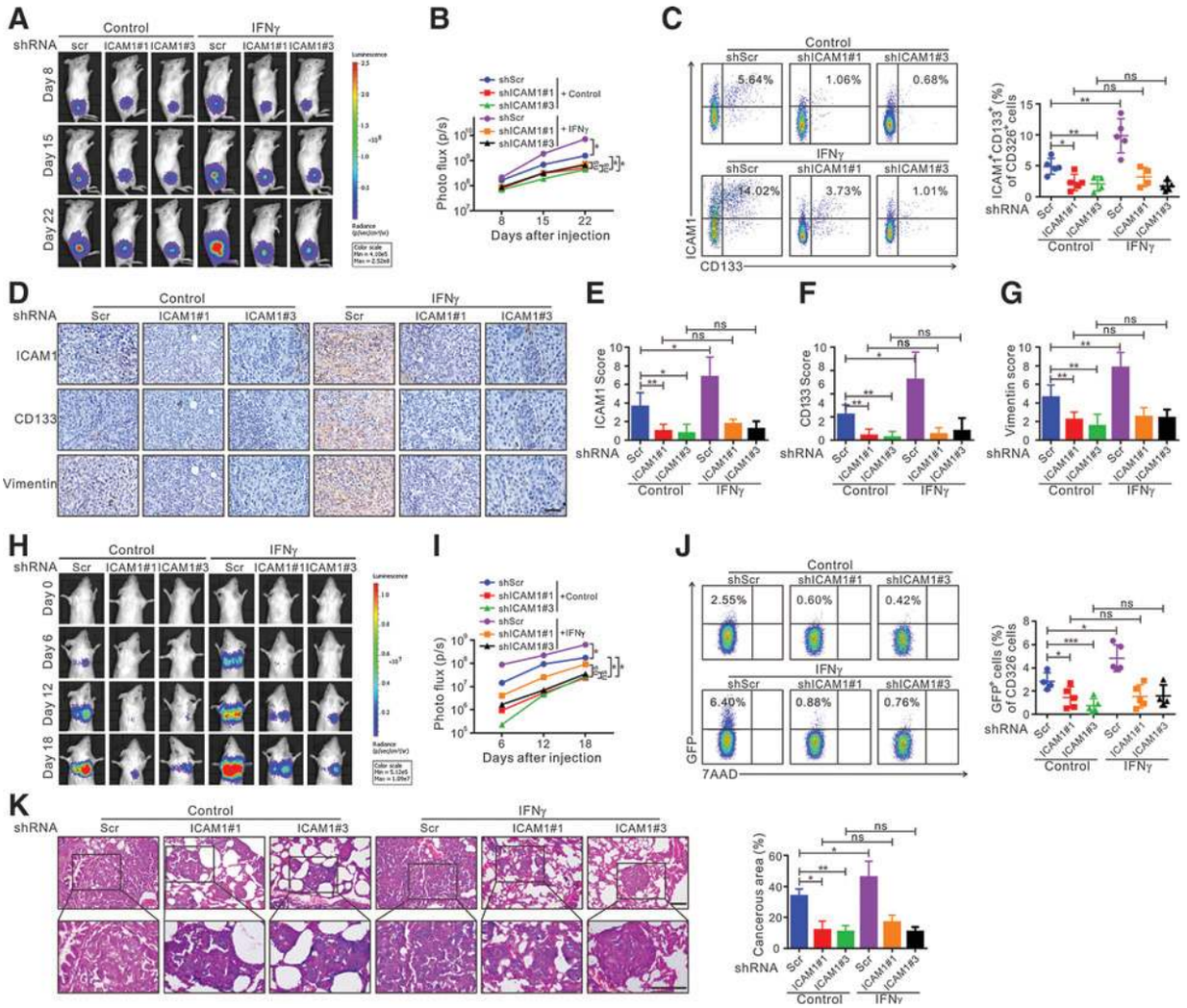

Figure 5.

Low-dose IFNγ promotes tumor growth and lung metastasis of NSCLC in an ICAM1-dependent manner. **A** and **B,** Tumor growth was measured at day 14, 21, and 28 after cell injection using *in vivo* imaging system. **C,** The frequency of ICAM1$^+$CD133$^+$ tumor cells of CD326$^+$ cells in mice-bearing xenografts was detected using flow cytometry. **D,** Consecutive sections of mice-bearing xenografts were used to analyze the coexpression levels of ICAM1, CD133, and vimentin by IHC staining. Scale bars, 50 μm. **E–G,** Scores of ICAM1, CD133, and vimentin in mice-bearing xenografts are shown as a statistical graph. **H** and **I,** Metastasis was evaluated using an *in vivo* imaging system at day 0, 6, 12, and 18 after injection. **J** and **K,** The lungs of the mice in each group were harvested at day 22 to analyze the frequency of GFP$^+$ NSCLC cells of CD326$^+$ cells by flow cytometry (**J**) and the metastatic nodules in the lungs by hematoxylin-eosin staining (**K**). Scale bars, 100 μm. The results are representative of three independent experiments. *, $P < 0.05$; **, $P < 0.01$; ***, $P < 0.001$; ns, not significant. Scr, Scramble.

stemness only in an IFNγ-low TME rather than in an IFNγ-high TME.

Discussion

Emerging evidence has reported that IFNγ may be involved in tumor progression, but the exact mechanism was not fully understood. In this study, we firstly identified the dose-dependent effect of IFNγ on tumor stemness in NSCLC. Low-dose IFNγ-induced tumor stemness via the ICAM1–PI3K–Akt–Notch1 axis, whereas high-dose IFNγ mainly mediated cell apoptosis through the JAK1–STAT1–caspase pathway (Fig. 6K).

IFNγ has a controversial role in regulating antitumor immunity. As there are few immunosuppressive factors in the TME in the early stage of solid tumor growth, effector T and NK cells can efficiently recognize tumor cells and subsequently produce high levels of IFNγ, resulting in the apoptosis of tumor cells. However, with tumor progression, T and NK cells become dysfunctional in the late stage (34), eventually generating an IFNγ-low TME. In addition, there is a reduction of T- and NK-cell infiltration in the center of cancer nest as well as those "cold tumors," which may also form an IFNγ-low niche, lacking effective immune infiltration. Low-level IFNγ is not sufficient to induce the apoptosis of a large number of tumor cells, which in turn accelerates tumor development through various mechanisms, such as the mediation of immunosuppression (7, 35–37), maintenance of CSCs dormancy (11), and induction of metastatic CSC generation (12). In this study, we clearly demonstrated that low-dose IFNγ endowed

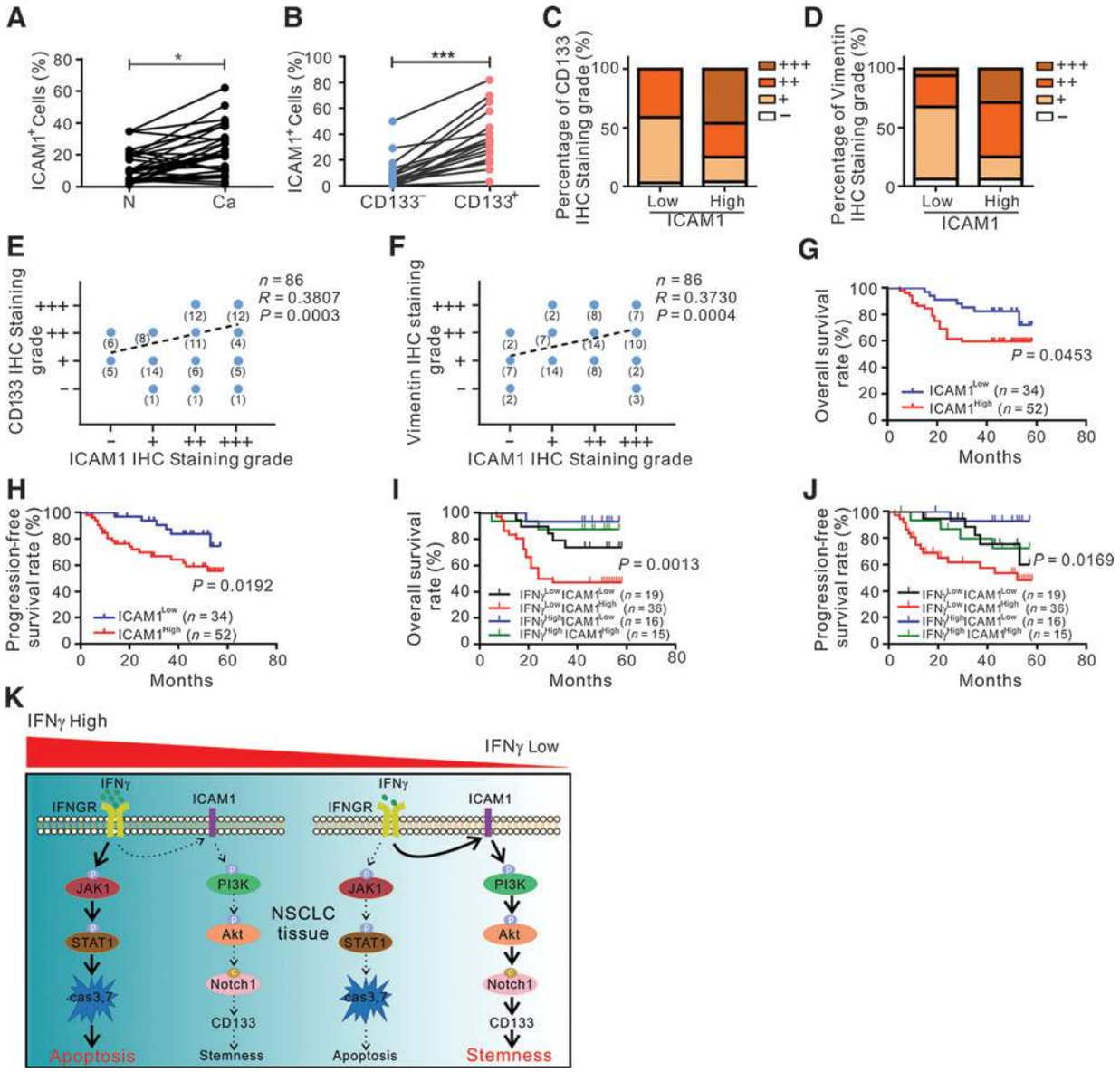

Figure 6.

ICAM1 is significantly upregulated by CD133$^+$ tumor cells and strongly correlated with a poor prognosis in patients with NSCLC. **A,** The frequency of ICAM1$^+$ cells in CD326$^+$ cells in tumor tissues and adjacent normal tissues was analyzed by flow cytometry ($n = 35$). **B,** The frequency of ICAM1$^+$ cells in CD326$^+$CD133$^-$ and CD326$^+$CD133$^+$ cells was analyzed by flow cytometry in NSCLC tissues ($n = 35$). **C** and **D,** The actual distribution of IHC results between ICAM1 and CD133 or vimentin expression in 86 NSCLC tissues. **E** and **F,** Spearman correlation analysis of the correlation between ICAM1 and CD133 or vimentin in 86 NSCLC specimens was performed according to the IHC staining results. **G–J,** Kaplan–Meier analysis of OS and progression-free survival in the 86 patients with NSCLC according to ICAM1 or both IFNγ and ICAM1 expression assessed by IHC staining. **K,** Schematic diagram. Log-rank tests were used in **G–J**. The results are representative of three independent experiments. *, $P < 0.05$; ***, $P < 0.0001$. c, cleaved; Ca, cancer tissue; cas, caspase; N, normal tissue; p, phosphorylation.

stem-like properties of tumor cells through the ICAM1–PI3K–Akt–Notch1 axis, while high-dose IFNγ mainly exerted antitumor effect via the JAK1–STAT1–caspase pathway in NSCLC. According to these findings, we infer that the regulation of low-level IFNγ on tumor stemness *in vivo* may be a spatial and temporal effect, which only occur in the time of in late-stage or in the sites lacking effective immune infiltration. Consistently, the function of low-level IFNγ in maintaining or promoting tumor stemness has also been reported in certain tumor models (11, 12). As we all know, IFNγ not only induces tumor cell apoptosis and stemness but also upregulates PD-L1 expression and activates MDSC to mediate immunosuppression (7, 35–37), which may induce cancer progression and interfere with low-dose IFNγ-induced cancer progression in immunocompetent mice. In addition, it is currently very difficult to precisely control the level of IFNγ in immunocompetent mice due to unknown IFNγ production in many cells and tissues. Taken all these points into account, we only verified our results *in vivo* by using immunodeficient mouse models in this

study, consistent with other studies on IFNγ regulating tumor cell growth (38–40).

Clinically, the adoptive transfer of receptor-engineered T cells and immune checkpoints blockade are still limited in treating some solid tumors (41–43). It was reported that low-dose IFNγ generated at the tumor site increases the risk of tumor metastasis during immunotherapy (9, 10). A recent study has reported that tumor stemness might cause PD-1/PD-L1 blockade resistance (44). In our view, the low-level IFNγ generated by dysfunctional T or NK cells in the TME may lead to treatment failure of immunotherapy by inducing tumor stemness. The dose of IFNγ delivered to the tumor site should be high when using IFNγ-based cancer immunotherapy. Accordingly, for adoptive T-cell therapy, a key issue is to ensure the effector function of T cells after reaching the tumor site, particularly when treating advanced solid tumors.

In this study, we found that ICAM1 merely mediated tumor stemness in the IFNγ-low rather than the IFNγ-high TME, and better survival was also observed in IFN $\gamma^{high}ICAM1^{high}$ patients that that in IFN $\gamma^{low}ICAM1^{high}$ patients. It may be necessary to evaluate the levels of IFNγ in the TME when using ICAM1-targeting therapy, as patients with low IFNγ levels may be more sensitive. However, ICAM1 was expressed on not only tumor cells but also a variety of stroma cells, such as endothelial cells. Thus, ICAM1 cannot be directly used as a specific target. ICAM1-targeting therapy may be applied by using nanoparticles encapsulating ICAM1 small-molecule inhibitor, such as silibinin. These nanoparticles may specifically deliver the ICAM1 inhibitor to tumor sites. In summary, low-dose IFNγ preferably induced tumor stemness via the ICAM1–PI3K–Akt–Notch1 axis, whereas high-dose IFNγ mainly mediated cell apoptosis through the JAK1–STAT1–caspase pathway in NSCLC. Inhibition of ICAM1 efficiently blocked the stem-like properties of tumor cells induced by low-dose IFNγ *in vitro* and *in vivo*. Our findings firstly revealed the dose-dependent effect of IFNγ in inducing tumor stemness and clearly elucidated the distinct molecular mechanisms activated by IFNγ in a dose-dependent manner, providing insights into cancer progression and treatment, particularly patients with low-level IFNγ expression in the TME.

Disclosure of Potential Conflicts of Interest

No potential conflicts of interest were disclosed.

Authors' Contributions

Conception and design: M. Song, Y. Ping, L. Yang, Z. Li, B. Zhang
Development of methodology: F. Li, S. Cheng, D. Yue, L. Wang
Acquisition of data (provided animals, acquired and managed patients, provided facilities, etc.): M. Song, K. Zhang, J. Qu, T. Sun, L. Wang
Analysis and interpretation of data (e.g., statistical analysis, biostatistics, computational analysis): M. Song, K. Zhang, C. Zhang, J. Qu, B. Zhang, L. Wang
Writing, review, and/or revision of the manuscript: M. Song, L. Yang, N.R. Maimela, Z. Li, J. Xia, B. Zhang, L. Wang
Administrative, technical, or material support (i.e., reporting or organizing data, constructing databases): F. Li, C. Zhang, S. Liu, L. Wang
Study supervision: L. Wang, Y. Zhang

Acknowledgments

This study was funded by the National Key R&D Program of China (2018YFC1313400 to J. Xia), the National Natural Science Foundation of China (grant nos. 81872410 and 81771781 to L. Wang and Y. Zhang, respectively), and the National Key Research and Development Program of China (2016YFC1303500 to T. Wan).

The costs of publication of this article were defrayed in part by the payment of page charges. This article must therefore be hereby marked *advertisement* in accordance with 18 U.S.C. Section 1734 solely to indicate this fact.

Received February 19, 2019; revised April 5, 2019; accepted May 8, 2019; published first May 13, 2019.

References

1. Tannenbaum CS, Hamilton TA. Immune-inflammatory mechanisms in IFNgamma-mediated anti-tumor activity. Semin Cancer Biol 2000;10:113–23.
2. Sadanaga N, Nagoshi M, Lederer JA, Joo HG, Eberlein TJ, Goedegebuure PS. Local secretion of IFN-gamma induces an antitumor response: comparison between T cells plus IL-2 and IFN-gamma transfected tumor cells. J Immunother 1999;22:315–23.
3. Platanias LC. Mechanisms of type-I- and type-II-interferon-mediated signalling. Nat Rev Immunol 2005;5:375–86.
4. Muller-Hermelink N, Braumuller H, Pichler B, Wieder T, Mailhammer R, Schaak K, et al. TNFR1 signaling and IFN-gamma signaling determine whether T cells induce tumor dormancy or promote multistage carcinogenesis. Cancer Cell 2008;13:507–18.
5. Murohashi I, Hoang T. Interferon-gamma enhances growth factor-dependent proliferation of clonogenic cells in acute myeloblastic leukemia. Blood 1991;78:1085–95.
6. Xiao M, Wang C, Zhang J, Li Z, Zhao X, Qin Z. IFNgamma promotes papilloma development by up-regulating Th17-associated inflammation. Cancer Res 2009;69:2010–7.
7. Ayers M, Lunceford J, Nebozhyn M, Murphy E, Loboda A, Kaufman DR, et al. IFN-gamma-related mRNA profile predicts clinical response to PD-1 blockade. J Clin Invest 2017;127:2930–40.
8. He YF, Wang XH, Zhang GM, Chen HT, Zhang H, Feng ZH. Sustained low-level expression of interferon-gamma promotes tumor development: potential insights in tumor prevention and tumor immunotherapy. Cancer Immunol Immunother 2005;54:891–7.
9. Kelly SA, Gschmeissner S, East N, Balkwill FR. Enhancement of metastatic potential by gamma-interferon. Cancer Res 1991;51:4020–7.
10. Gong W, Zhang GM, Liu Y, Lei Z, Li D, Yuan Y, et al. IFN-gamma withdrawal after immunotherapy potentiates B16 melanoma invasion and metastasis by intensifying tumor integrin alphavbeta3 signaling. Int J Cancer 2008;123:702–8.
11. Liu Y, Liang X, Yin X, Lv J, Tang K, Ma J, et al. Blockade of IDO-kynurenine-AhR metabolic circuitry abrogates IFN-gamma-induced immunologic dormancy of tumor-repopulating cells. Nat Commun 2017;8:15207.
12. Chen HC, Chou AS, Liu YC, Hsieh CH, Kang CC, Pang ST, et al. Induction of metastatic cancer stem cells from the NK/LAK-resistant floating, but not adherent, subset of the UP-LN1 carcinoma cell line by IFN-gamma. Lab Invest 2011;91:1502–13.
13. Batlle E, Clevers H. Cancer stem cells revisited. Nat Med 2017;23:1124–34.
14. Takebe N, Miele L, Harris PJ, Jeong W, Bando H, Kahn M, et al. Targeting Notch, Hedgehog, and Wnt pathways in cancer stem cells: clinical update. Nat Rev Clin Oncol 2015;12:445–64.
15. Mani SA, Guo W, Liao MJ, Eaton EN, Ayyanan A, Zhou AY, et al. The epithelial-mesenchymal transition generates cells with properties of stem cells. Cell 2008;133:704–15.
16. Plaks V, Kong N, Werb Z. The cancer stem cell niche: how essential is the niche in regulating stemness of tumor cells? Cell Stem Cell 2015;16:225–38.
17. Qiao Y, Zhang C, Li A, Wang D, Luo Z, Ping Y, et al. IL6 derived from cancer-associated fibroblasts promotes chemoresistance via CXCR7 in esophageal squamous cell carcinoma. Oncogene 2017;37:873–83.
18. Lawson C, Wolf S. ICAM-1 signaling in endothelial cells. Pharmacol Rep 2009;61:22–32.
19. Duperray A, Languino LR, Plescia J, McDowall A, Hogg N, Craig AG, et al. Molecular identification of a novel fibrinogen binding site on the first

domain of ICAM-1 regulating leukocyte-endothelium bridging. J Biol Chem 1997;272:435–41.
20. Millan J, Hewlett L, Glyn M, Toomre D, Clark P, Ridley AJ. Lymphocyte transcellular migration occurs through recruitment of endothelial ICAM-1 to caveola- and F-actin-rich domains. Nat Cell Biol 2006;8:113–23.
21. Kanters E, van Rijssel J, Hensbergen PJ, Hondius D, Mul FP, Deelder AM, et al. Filamin B mediates ICAM-1-driven leukocyte transendothelial migration. J Biol Chem 2008;283:31830–9.
22. Rothlein R, Czajkowski M, O'Neill MM, Marlin SD, Mainolfi E, Merluzzi VJ. Induction of intercellular adhesion molecule 1 on primary and continuous cell lines by pro-inflammatory cytokines. Regulation by pharmacologic agents and neutralizing antibodies. J Immunol 1988;141:1665–9.
23. Chen CC, Chen JJ, Chou CY. Protein kinase calpha but not p44/42 mitogen-activated protein kinase, p38, or c-Jun NH(2)-terminal kinase is required for intercellular adhesion molecule-1 expression mediated by interleukin-1beta: involvement of sequential activation of tyrosine kinase, nuclear factor-kappaB-inducing kinase, and IkappaB kinase 2. Mol Pharmacol 2000;58:1479–89.
24. Liu S, Li N, Yu X, Xiao X, Cheng K, Hu J, et al. Expression of intercellular adhesion molecule 1 by hepatocellular carcinoma stem cells and circulating tumor cells. Gastroenterology 2013;144:1031–41.
25. Tsai ST, Wang PJ, Liou NJ, Lin PS, Chen CH, Chang WC. ICAM1 is a potential cancer stem cell marker of esophageal squamous cell carcinoma. PLoS One 2015;10:e0142834.
26. Huang C, Li N, Li Z, Chang A, Chen Y, Zhao T, et al. Tumour-derived interleukin 35 promotes pancreatic ductal adenocarcinoma cell extravasation and metastasis by inducing ICAM1 expression. Nat Commun 2017;8:14035.
27. Min IM, Shevlin E, Vedvyas Y, Zaman M, Wyrwas B, Scognamiglio T, et al. CAR T therapy targeting ICAM-1 eliminates advanced human thyroid tumors. Clin Cancer Res 2017;23:7569–83.
28. Levina V, Marrangoni AM, DeMarco R, Gorelik E, Lokshin AE. Drug-selected human lung cancer stem cells: cytokine network, tumorigenic and metastatic properties. PLoS One 2008;3:e3077.
29. Lin YC, Shun CT, Wu MS, Chen CC. A novel anticancer effect of thalidomide: inhibition of intercellular adhesion molecule-1-mediated cell invasion and metastasis through suppression of nuclear factor-kappaB. Clin Cancer Res 2006;12:7165–73.
30. Eil R, Vodnala SK, Clever D, Klebanoff CA, Sukumar M, Pan JH, et al. Ionic immune suppression within the tumour microenvironment limits T cell effector function. Nature 2016;537:539–43.
31. Roy S, Lu K, Nayak MK, Bhuniya A, Ghosh T, Kundu S, et al. Activation of D2 dopamine receptors in CD133+ve cancer stem cells in non-small cell lung carcinoma inhibits proliferation, clonogenic ability, and invasiveness of these cells. J Biol Chem 2017;292:435–45.
32. Zakaria N, Satar NA, Abu Halim NH, Ngalim SH, Yusoff NM, Lin J, et al. Targeting lung cancer stem cells: research and clinical impacts. Front Oncol 2017;7:80.
33. Ohtsuka T, Ishibashi M, Gradwohl G, Nakanishi S, Guillemot F, Kageyama R. Hes1 and Hes5 as notch effectors in mammalian neuronal differentiation. EMBO J 1999;18:2196–207.
34. Chauvin JM, Pagliano O, Fourcade J, Sun Z, Wang H, Sander C, et al. TIGIT and PD-1 impair tumor antigen-specific CD8(+) T cells in melanoma patients. J Clin Invest 2015;125:2046–58.
35. Katz JB, Muller AJ, Prendergast GC. Indoleamine 2,3-dioxygenase in T-cell tolerance and tumoral immune escape. Immunol Rev 2008;222:206–21.
36. Spranger S, Spaapen RM, Zha Y, Williams J, Meng Y, Ha TT, et al. Up-regulation of PD-L1, IDO, and T(regs) in the melanoma tumor microenvironment is driven by CD8(+) T cells. Sci Transl Med 2013;5:200ra116.
37. Gato-Canas M, Zuazo M, Arasanz H, Ibanez-Vea M, Lorenzo L, Fernandez-Hinojal G, et al. PDL1 signals through conserved sequence motifs to overcome interferon-mediated cytotoxicity. Cell Rep 2017;20:1818–29.
38. Twentyman PR, Workman P, Wright KA, Bleehen NM. The effects of alpha and gamma interferons on human lung cancer cells grown in vitro or as xenografts in nude mice. Br J Cancer 1985;52:21–9.
39. Balkwill FR, Moodie EM, Freedman V, Fantes KH. Human interferon inhibits the growth of established human breast tumours in the nude mouse. Int J Cancer 1982;30:231–5.
40. Liu H, Golji J, Brodeur LK, Chung FS, Chen JT, deBeaumont RS, et al. Tumor-derived IFN triggers chronic pathway agonism and sensitivity to ADAR loss. Nat Med 2019;25:95–102.
41. Daud AI, Loo K, Pauli ML, Sanchez-Rodriguez R, Sandoval PM, Taravati K, et al. Tumor immune profiling predicts response to anti-PD-1 therapy in human melanoma. J Clin Invest 2016;126:3447–52.
42. Huang X, Yang Y. Driving an improved CAR for cancer immunotherapy. J Clin Invest 2016;126:2795–8.
43. Ping Y, Liu C, Zhang Y. T-cell receptor-engineered T cells for cancer treatment: current status and future directions. Protein Cell 2018;9:254–66.
44. Zou W, Wolchok JD, Chen L. PD-L1 (B7-H1) and PD-1 pathway blockade for cancer therapy: mechanisms, response biomarkers, and combinations. Sci Transl Med 2016;8:328rv4.